J. Innovative Eng. Nat. Sci., vol. 3, no. 2, pp. 153-166, 2023.
http://dx.doi.org/10.29228/JIENS.70059

Journal of Innovative Engineering and Natural Science
(Yenilikçi Mühendislik ve Doğa Bilimleri Dergisi)
journal homepage: https://jiens.org

Original Paper

Detecting acetone from breath using a $PrFeO_3$-doped PANi/TiO_2-coated PAN nanofiber sensor for non-invasive diabetic diagnosis

Nesibe Yeşildağ[a], Ömer Faruk Ünsal[a], Ramazan Gömeç[b] and Ayşe Çelik Bedeloğlu[a,*]

[a]*Department of Polymer Materials Engineering, Bursa Technical University, Eflak Str. No: 177 Yıldırım, Bursa, 16310, Turkey.*
[b]*Aydın Textile, İkitelli Organized Industrial Zone, Eski Turgut Özal Str. No: 38/3 Başakşehir, İstanbul, 34490, Turkey.*

ARTICLE INFO

Article history:
Received 15 May 2023
Received in revised form 4 July 2023
Accepted 6 July 2023

Available online

Keywords:
Nanofiber
Acetone
Gas sensor
Non-invasive
Diabetics
Perovskites

ABSTRACT

Polyacrylonitrile (PAN) nanofibers doped with varying concentrations of perovskite praseodymium ferrite ($PrFeO_3$) nanoparticles synthesized by calcination were successfully manufactured using a simple electrospinning process. The nanofibers were coated with layers of polyaniline-titanium dioxide (PANi-TiO_2) combination using an air brush. The structure, morphology, and electrical characteristics of the nanoparticles and nanofibers were characterized by SEM, FT-IR, and electrical measurement methods. The results indicated that the produced nanofibers exhibited a strong in vitro interaction and selectivity against acetone gas, a biomarker of diabetes. Perovskite nanoparticle doped PAN nanofibers have shown approximately 43% change in resistance with acetone gas exposure. These findings suggest that $PrFeO_3$-doped nanofibers hold promise as potential candidates for acetone gas sensors in non-invasive diabetes monitoring.

I. INTRODUCTION

According to reports from the International Diabetes Federation (IDF) [1], there are currently over 537 million adults living with diabetes worldwide, with one in every 10 individuals being affected by the disease. Reports from the World Health Organization (WHO) [2], estimate that there are 422 million adults with diabetes (ages 18-99), with an expected increase to 629 million by 2045 [3, 4]. The number of recorded deaths from diabetes is currently at 1.6 million annually [5]. The rising prevalence of diabetes highlights the increasing yearly medical and non-medical costs, as well as the growing number of diabetic fatalities [4, 6]. Diabetes Mellitus (DM) is a metabolic disorder characterized by hyperglycemia (blood glucose level greater than 230 mg/dL) or hypoglycemia (blood glucose level less than 65 mg/dL) caused by insulin hormone secretion or activation problems [4, 7]. Diabetes is caused by the pancreas's failure to produce enough insulin for the body or the body's inability to use the insulin produced by the pancreas effectively. Type 1 Diabetes Mellitus (T1DM) is a metabolic disorder caused by the destruction of cells in the pancreas as a result of the immune system recognizing and attacking the beta cells as foreign, resulting in insulin deficiency. Type 2 Diabetes Mellitus (T2DM) is caused by the body's inability to use insulin effectively. Other types of diabetes include genetic disorders, drug use, genetic syndromes, and gestational diabetes (GDM) [4, 8–12]. When T1DM and T2DM patients cannot effectively absorb glucose from circulation, the metabolic shift results in increased ketone synthesis in the blood (ketonemia), urine (ketonuria), and breath (ketosis) [13]. Acetone in the breath has been identified as an effective biomarker [5]. While it is evident that

*Corresponding author. Tel.: +90-224-300-3491; e-mail: ayse.bedeloglu@btu.edu.tr

T1DM patients have a high concentration of ketones in their breath, there is no universally accepted measure of the concentration of ketones in T2DM patients' breath [14–21].

Clinical investigations have demonstrated that the concentration of acetone in the breath of individuals with diabetes exceeds 1.8 ppm (with a range of 1.25-2.5 ppm), while healthy individuals exhibit acetone concentration below 0.9 ppm (with a range of 0.2-1.8 ppm) [22–27]. Moreover, the concentration of acetone in the breath of individuals with type 1 diabetes mellitus (T1DM) may reach up to 25 ppm [5, 24, 28–30]. In terms of age, healthy adults between the ages of 40-50 exhibit acetone concentration of 0.2-0.8 ppm in their breath, while adult diabetics aged 50 or older exhibit acetone concentration within the range of 1.8 ppm [3]. The significant difference in acetone concentration between healthy individuals and diabetics makes acetone in the breath a valuable biomarker for diabetes identification [26, 27, 29, 31]. The discovery of the odor of rotten apple breath by John Gallo in 1798 and the identification of this odor as acetone in 1857 led to the use of acetone as the first biomarker for diabetes [5, 24, 31]. In 1971, Linus Pauling presented a report proposing a study plan for differentiating 250 gases in human breath using gas chromatography [5, 32]. Since then, more than 3000 distinct volatile organic compounds (VOCs) and aerosolized particles have been identified in human breath [32–34]. These gases are produced as byproducts of metabolic reactions, for physiological functions such as cell-to-cell communication, or in infections and other pathological conditions in the body [32]. Diet [35, 36], exercise [37], and medical condition [5, 20, 38] all contribute to variations in breath acetone content. In addition to diabetes, intensive physical active ity and ketogenic diets may also cause an increase in breath acetone content. Therefore, the measurement of acetone in breath is critical for diabetes diagnosis and monitoring the efficacy of therapies in medical disorders [17]. is considered a hazardous gas as well as a breath biomarker for diabetes [3, 39, 40], as it can cause nausea in humans above 2000 ppm and respiratory irritation above 300-500 ppm [3, 40].

Elevated blood sugar levels in the body lead to several health complications, including hyperglycemia, cardiovascular disease, diabetic nephropathy, diabetic retinopathy, and diabetic neuropathy [41, 42]. Furthermore, diabetes can also result in heart attack, stroke, blindness, kidney failure, leg amputation, vision loss, and nerve damage [2, 5, 42]. These complications highlight the critical importance of controlling blood sugar levels [3, 43]. To diagnose diabetes, a Plasma Glucose Level test is necessary. Diabetics receiving insulin therapy for diabetes management need to test their blood glucose levels at least three times per day using the conventional finger prick method [32, 44, 45]. However, these tests have significant drawbacks such as being uneconomical, unsafe, impractical, painful, laborious, and susceptible to the risk of infection. These drawbacks can be eliminated by using the acetone analysis method from breath. Breath analysis is a powerful tool in medical diagnosis and disease research due to its noninvasive nature and real-time monitoring capability [16, 18, 24, 32–34, 46–48]. Various techniques have been employed to measure acetone concentration for breath analysis, including mass spectrometry (MS), proton transfer reaction by mass spectrometry (PTR-MS), gas chromatography (GC), flame ionization detector (FID), selected ion flow tube mass spectrometry, ion mobility spectrometry (IMS), among others [47, 49–51]. Nonetheless, these sensitive and reliable techniques have certain limitations such as bulky equipment size, high cost, and unsuitability for miniaturization, making them unsuitable for daily diabetes monitoring [52].

An alternative approach to the diagnosis and monitoring of diabetes is the use of sensors for non-invasive and continuous real-time measurement of acetone in breath. This method has the potential to facilitate early treatment and promote effective management of the disease [3, 32]. Chemical sensors have become increasingly popular for

breath analysis due to their small size, portability, and ability to provide real-time monitoring at a low cost. In recent years, sensors that are selective, sensitive, stable, robust, and economical have been developed for breath analysis. The advantages of using chemical sensors include ease of use, ease of sampling, and the ability to obtain measurements from unconscious patients [32, 53].

Chemical gas sensors function by changing one or more physical properties, such as mass, electrical conductivity, or dielectric properties when exposed to gas molecules [5]. Chemical gas sensors operate by measuring the change in electrical resistance of the sensing material in the presence of target analytes and translating this chemical information by changing the electrical resistance [5, 54]. Recently, chemical-resistant gas sensors have been developed for the detection of acetone gas, a biomarker of diabetes, from breath [3, 55]. The detection mechanisms of these sensors based on change in electrical resistance of sensing material by the molecular and/or crystalline structure change. The basis for determining the presence of acetone is the reactions between surface oxygen and acetone gas [3, 56]. The performance of these sensors is affected by various features such as surface area, particle size, crystal defects, porous structures, stoichiometry, and morphology [56–58].

In recent years, there has been increasing interest in the development of chemical resistance gas sensors using semiconductor metal oxides for acetone detection. Among the most extensively studied materials for chemical resistance sensors are WO_3, ZnO, SnO_2, Fe_2O_3, In_2O_3, TiO_2, perovskites, and p-type metal oxides. TiO_2, in particular, has proven to be effective in sensing various gases [59]. Furthermore, environmentally friendly perovskites have demonstrated exceptional long-term stability and durability in the detection area due to their stable lattice structure [30, 60–63]. Perovskites such as Pd-doped $SmFeO_3$ [64], $SmFeO_3$/ZnO (p-$SmFeO_3$/n-ZnO) [64], Ni-doped $LaFeO_3$ [65] and Pd-doped $NdFeO_3$ [66] have been investigated, with the gas sensitivity performance of praseodymium ferrite ($PrFeO_3$) receiving particular attention. In one study, Ma et al. (2017) [67] investigated the structure, elemental composition, and morphology of $PrFeO_3$ hollow nanofibers. These nanofibers exhibited a low operating temperature (180 ℃), high response value, good selectivity, fast response recovery, and excellent long-term stability [67]. As such, $PrFeO_3$ hollow nanofibers have the potential to be used in the fabrication of high-performance acetone sensors and represent promising candidates for practical applications. In a subsequent study, Ma et al. (2020) [68] investigated Sm^{3+} doped $PrFeO_3$ to improve the response and recovery process of $PrFeO_3$ gas sensors. Nanofibers have become increasingly relevant in the sensing configuration of biosensors, as their use can reduce sensor size, increase surface energy, and improve sensitivity by increasing specific surface area [69–71]. Conducting polymers, such as polyaniline (PANi), can also be utilized in the sensing configuration of gas sensors [72], where their molecular and macroscopic properties can change when exposed to various chemicals [73]. PANi has been used as a sensing material for gases such as hydrogen (H_2), ammonia (NH_3), nitrogen oxide (NO_2), hydrogen sulfide (H_2S), dimethylamine (DMA), and liquid petroleum gas (LPG) in various forms [74]. Therefore, this study sought to combine conductive polymers, metal oxides, perovskites, and nanofibers to create a unique sensor structure with the advantages of ease of synthesis, good environmental and chemical stability, and improved sensing properties. Specifically, the study employed crystal lattice structured perovskite $PrFeO_3$ nanoparticles on PANi-TiO_2-coated PAN nanofibers to develop an efficient acetone sensor for diabetics, followed by structural, morphological, and electrochemical characterizations.

II. EXPERIMENTAL METHOD

2.1 Materials

Praseodymium (III) nitrate hydrate (99.9%, $Pr(NO_3)_3.H_2O$) (REO, Alfa Aesar, M=326.92 g/mol), Iron (III) nitrate nonahydrate ($Fe(NO_3)_3.9H_2O$) (Sigma Aldrich, Merk, M=403.95 g/mol), Citric acid monohydrate (98%, $C_6H_8O_7.H_2O$) (food grade, Aromel, M=210.14 g/mol) and urea (≥ 99.5%, CH_4N_2O) (Iso-lab) were used for synthesis of perovskite praseodymium ferrite ($PrFeO_3$). Aniline (99%, $C_6H_5NH_2$) (Sigma Aldrich), Ammonium persulfate (≥98%, APS) ($H_8N_2O_8S_2$) (Honeywell / Fluka, M=228.2 g/mol), extra pure hydrochloric acid (30-32%, HCl(aq)) (TEKKİM), Titanium (IV) oxide (≥99.5%, TiO_2) (particle size 21 nm, Sigma Aldrich, M=79.87 g/mol) and ethanol (C_2H_5OH) were used for synthesis of titanium dioxide-doped polyaniline (PANi). Polyacrylonitrile (PAN) (MW=150,000, JK Chemical) and N,N dimethyl formamide (99.9%, DMF) as solvent (Carlo Erba Reagents, M=73.1 g/mol) was used for preparation of PAN nanofiber.

2.2 Methods

2.2.1. Synthesis of Praseodymium Ferrite ($PrFeO_3$), Polyaniline (PANi) and Titanium (IV) oxide (TiO_2)

The $PrFeO_3$ nanoparticles were synthesized using the sol-gel process, which has been previously reported in the literature [75]. To prepare the growth solution at room temperature, a solution containing 0.1 M $Pr(NO_3)_3$ and 0.67 M citric acid was used, and a separate 0.1 M solution of iron (III) nitrate was prepared. $Fe(NO_3)_3$ solution was then added dropwise to the growth solution until the molar ratio of $Pr(NO_3)_3$ to $Fe(NO_3)_3$ in the solution became 1:1. To obtain a gel, 0.5 g of urea was added to the resulting solution, which was stirred in a 50°C water bath for 60 minutes. The gel was then kept at 80°C for 24 hours to obtain the xerogel, which was calcined at 800°C for 5 hours to produce the cinnamon-colored nanoparticles (Figure 1).

Figure 1. Picture of synthesized $PrFeO_3$

For the synthesis of PANi-TiO_2, 3.75 mL of aniline ($C_6H_5NH_2$) as the monomer and a desired amount of TiO_2 (30 wt.%) were added to the mixture and ultrasonicated until the TiO_2 nanoparticles were uniformly dispersed. Then, 2.360 g of ammonium persulfate ($(NH_4)_2S_2O_8$) prepared as an initiator was added dropwise in a cold water bath to the solution obtained by dissolving in 100 mL of 1 M hydrochloric acid (HCl). The solution was kept in a cold water bath under magnetic stirring condition for approximately 24 hours, until the polymerization was completed, resulting in a solution that changed from colorless to blue tones. The solution was filtered by vacuum filtration method, and the resulting PANi was washed twice with water (H_2O) and ethanol (C_2H_5OH), respectively [76]. The

dark green precipitate obtained after washing was taken into ethanol, and the concentration of PANi obtained was determined to be 11mg/L. Titanium (IV) oxide was weighed to 30% by mass and added to PANi as a powder. The solid amount in 2.5 mL of PANi/ethanol solution was determined to be 25 mg.

2.2.2. Preparation of Nanofibers and Air-Brush Coating Process

To produce nanofiber solutions, 5% (w%) solid polymer was dissolved in DMF, and after adding $PrFeO_3$, a total of 10 g of polymer solution containing 0%, 5%, 10%, and 20% $PrFeO_3$ was sonicated for 20 minutes. The resultant colloidal solution was covered with aluminum (Al) foil and paraffin tape to protect it from light. The nanofibers were then electrospun in the Nanospinner 24 device (Inovenso, NS24) at 28 kV, 500 rpm, and 175 mm between the nozzle and the collector.

Undoped PAN nanofiber, 5% $PrFeO_3$-added PAN nanofiber, 10% $PrFeO_3$-added PAN nanofiber, and 20%-$PrFeO_3$ added PAN nanofiber were coated with layers of PANi/TiO_2 using an air-brush method to a thickness of a few tens of microns. The coating was carried out by spraying at a pressure of 1-1.5 bar from a distance of 3 cm. The coated nanofibers were dried in a desiccator for approximately 48 hours.

2.2.3. Device fabrication

To construct the acetone sensor, the PANi/TiO_2 layer was coated on electrospun PAN nanofibers doped with $PrFeO_3$. Two copper electrodes were placed on the surface of the nanofiber sensor that was coated with the PANi/TiO_2 layer, with a distance of 1 cm between them. The produced nanofiber sensor was then heated in an oven at 40°C overnight to ensure complete moisture evaporation. The acetone sensing measurement was performed by modifying the following reference [77] in the air. To measure the acetone sensing characteristics, the sensors (Figure 2) were positioned at a distance of 10 cm from the petri dish in the sample holder, with the coated surface facing the acetone. The gas response of the nanofibers, measured as electrical resistance, was used to evaluate the acetone-sensing properties. The initial resistance of the nanofiber sensor was measured without acetone evaporation using a two-probe technique. Subsequently, acetone gas was heated using a hot plate to control acetone evaporation by maintaining a temperature between 50-55 °C, which is close to the acetone evaporation temperature. After 10 seconds, the second electrical resistance was measured.

2.2.4. Characterization

The morphology of $PrFeO_3$ nanoparticles, as well as the undoped and $PrFeO_3$-doped PAN nanofibers, were examined using a scanning electron microscope (SEM) (Carl Zeiss/Gemini 300) at different distances ranging from 8-9 mm and under a voltage of 5 kV. The bound structures of $PrFeO_3$ nanoparticles, undoped and $PrFeO_3$-doped PAN nanofiber structures were analyzed using an FT-IR spectrophotometer (Thermofisher NICOLET–iS50). The sensing measurements of PANi/TiO_2-coated $PrFeO_3$-doped PAN nanofibers were conducted through a two-point resistance measurement test in vitro using a multimeter (Keithley 2400 device).

Figure 2. PrFeO3-doped PANi/TiO_2-coated PAN sensor

III. RESULTS AND DISCUSSIONS

3.1 FT-IR Results

The results of the FT-IR analysis of $PrFeO_3$ nanoparticles are presented in Figure 3a. The spectrum revealed prominent absorption peaks at 462 cm^{-1}, which correspond to O-Fe-O bending vibrations, and 530 cm^{-1}, which correspond to Fe-O stretching vibrations [78]. In Figure 3b, the FT-IR spectra of undoped and $PrFeO_3$-doped PAN nanofibers are presented.

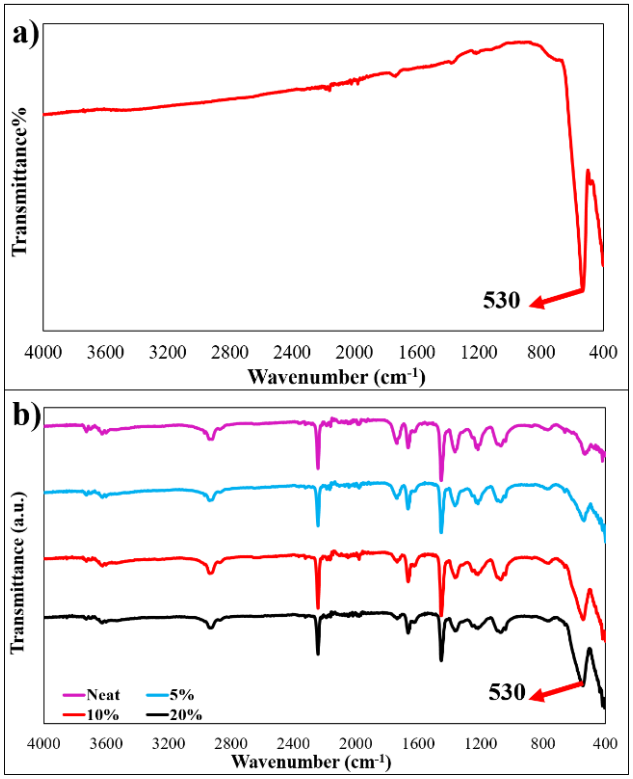

Figure 3. a) FT-IR results of $PrFeO_3$ nanoparticles and b) FT-IR results of undoped and $PrFeO_3$-doped PAN nanofiber structures

The Fe-O stretching peak of $PrFeO_3$ observed at 530 cm^{-1} became more prominent as the $PrFeO_3$ concentration increased, as seen from the FT-IR spectra of the undoped and $PrFeO_3$-doped PAN nanofiber structures. The effect of acetone treatment on powder $PrFeO_3$, undoped PAN nanofiber, and $PrFeO_3$-doped nanofiber was examined by

FT-IR analysis, and it was observed that the structure retained acetone (Figure 4). Although no significant change was observed in the FT-IR spectrum of powder $PrFeO_3$ after acetone treatment, the CO_2-induced peaks that appeared in the calcination range of 1200-1500 cm^{-1} disappeared [78]. In undoped PAN nanofiber, it was observed that the nanofiber porous structure held acetone, and the vibrations of the aliphatic -CH groups at 1217 and 1364 cm^{-1} of the PAN [79] were intensified by combining with the -CH vibrations of the acetone at the same points, indicating that the structure retained acetone.

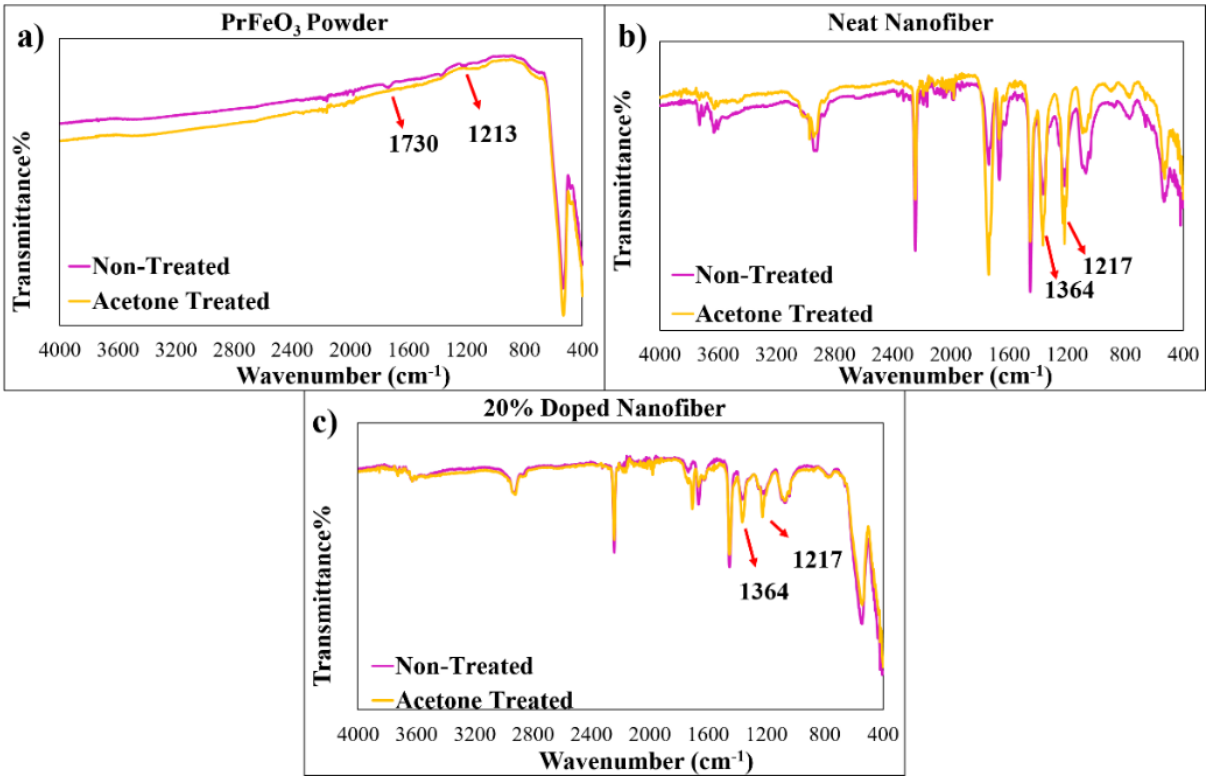

Figure 4. FT-IR spectra of undoped and $PrFeO_3$-doped PAN nanofiber structures

3.2 Morphology

Figure 5 displays SEM images of neat PAN nanofibers and $PrFeO_3$-doped PAN nanofibers before PANi-TiO_2 coating. The SEM images indicate that the nanofibers were formed uniformly with diameters ranging from 200 to 500 nm. Mean Diameters or neat nanofibers and 20% $PrFeO_3$ doped nanofibers were 336 nm and 216 nm, respectively (Figure 5a). Here, main reason that caused to thinning the fibres by nanoparticle loading into electrospinning solution was the decrease in polymer concentration. With the other words, while the polymer concentration was 5% by weight for neat PAN solution, the polymer concentration remained 4% since inorganic was loaded in 20% doped solution. Moreover, $PrFeO_3$ nanoparticles were observed to exist in the PAN nanofiber structure, with some embedded in the fibers and others protruding out of the fiber. The size of the nanoparticles was between 100 and 500 nanometers, and the addition of $PrFeO_3$ nanoparticles led to a decrease in the mean diameter of the PAN nanofibers (Figure 5b). The SEM images indicated that perovskite ($PrFeO_3$) nanoparticles were successfully produced using the sol-gel method. However, it was observed that the crystal particles were

fused and sintered together during calcination, resembling coral (Figure 5c). Despite this, the heat treatment synthesis method offers several advantages such as low cost, simplicity, low reaction temperatures, and no waste by-product [63,64,80].

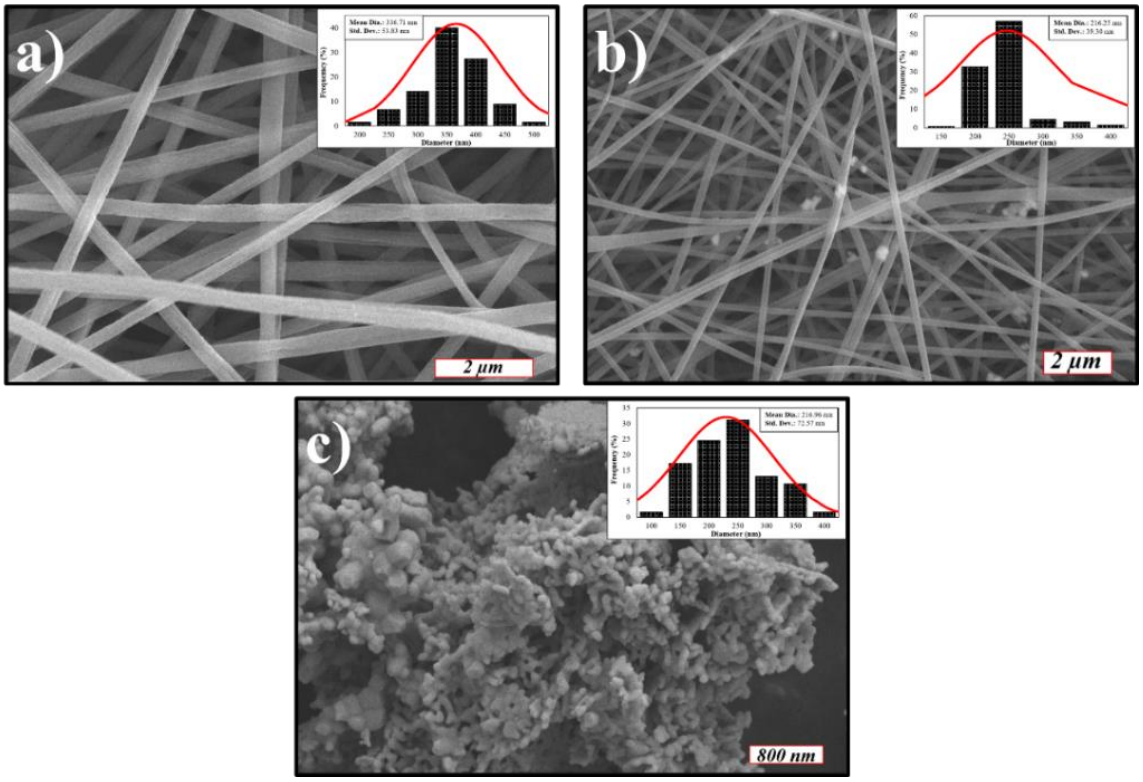

Figure 5. a) Undoped PAN nanofibers - b) 20% $PrFeO_3$-doped PAN nanofibers - c) $PrFeO_3$ nanoparticles

3.3 Sensing Measurements

Air-stable $PrFeO_3$, a perovskite material, possesses desirable sensing properties, including high response, good selectivity, and low operating temperatures, owing to its large specific surface area and abundance of active sites that facilitate gas molecule diffusion and adsorption, thereby enhancing its detection ability [81]. The gas sensing mechanism of $PrFeO_3$ is primarily based on the electrical resistance change before and after exposure to the test gas [67]. The use of electrospun nanofibers with high specific surface area and web-like morphology resulted in high sensing performance, as the target acetone gas molecules could diffuse efficiently into the nanofibers [82]. When the undoped PAN nanofiber sensor was exposed to acetone gas, its electrical resistance increased from 38.86 kΩ to 42 kΩ (Figure 6). Conversely, the electrical resistance of 5%, 10%, and 20% $PrFeO_3$-doped PAN nanofibers increased from 131.52 kΩ to 145.56 kΩ, 156.87 kΩ to 172.35 kΩ, and 508.5 kΩ to 726.6 kΩ, respectively, upon exposure to acetone gas (Figure 6). The observed increase in the ratio of $PrFeO_3$ in the nanofibers correspondingly increased the initial resistance of the sensors compared to the neat nanofibers. The results obtained are consistent with prior studies, which have shown that the electrical resistance of prepared sensors increases upon exposure to acetone gas [67]. Moreover, this increase is below 10% for undoped, 5%, and 10%-doped nanofibers, while the increase is approximately 30% for 20%-doped nanofiber sensors.

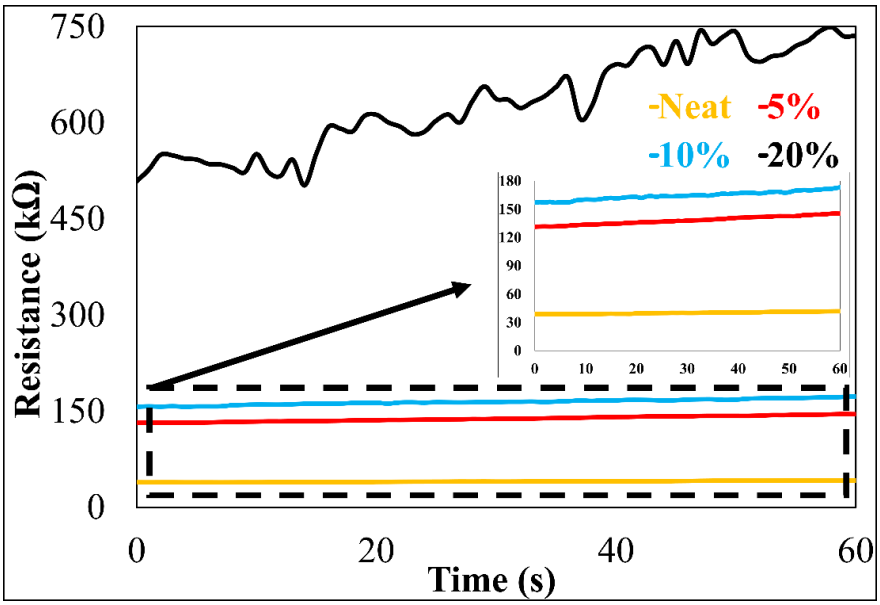

Figure 6. Electrical resistance change of PAN nanofiber sensors during acetone exposure

IV. CONCLUSIONS

In this study, $PrFeO_3$-doped PANi/TiO_2 coated PAN nanofibers were synthesized via a combination of $PrFeO_3$ synthesis, electrospinning of nanofibers, and air-brush coating. SEM images were obtained to confirm the successful synthesis and incorporation of $PrFeO_3$ nanoparticles into the PAN nanofiber structure. The electrical resistance of both doped and undoped nanofiber sensors increased when exposed to acetone gas, with the increase in resistance being more pronounced for doped nanofiber sensors as the amount of $PrFeO_3$ additive increased. Overall, these findings suggest that $PrFeO_3$-doped PANi/TiO_2 coated PAN nanofibers hold significant potential for use as high-performance acetone sensors, and may prove to be promising candidates for non-invasive detection of diabetes.

ACKNOWLEDGMENT

This project was supported under the project application number TUBITAK BIDEB 1139B411901869 within the scope of TUBITAK 2209-B Industry Oriented Research Project Support Programme for Undergraduate Students. This article is based upon work from COST Action “European Network to connect research and innovation efforts on advanced Smart Textiles” (CONTEXT, Ref. CA17107, https://www.context-cost.eu) supported by COST (European Cooperation in Science and Technology, https://www.cost.eu).

REFERENCES

[1] Webber S, International Diabetes Federation - Diabetes Atlas, 10th Edition 2021, 2013. https://doi.org/10.1016/j.diabres.2013.10.013.
[2] World Health Organization, Global Report on Diabetes, Isbn. 978 (2016) 88. https://doi.org/ISBN 978 92 4

156525 7.
[3] Baharuddin AA, Ang BC, Haseeb ASMA, Wong YC, Wong YH (2019) Advances in chemiresistive sensors for acetone gas detection. Materials Science in Semiconductor Processing 103 104616 https://doi.org/10.1016/j.mssp.2019.104616.
[4] Shokrekhodaei M and Quinones S (2020) Review of Non-Invasive Glucose Sensing Techniques. Sensors (Switzerland) 1251 https://sci-hub.scihubtw.tw/10.3390/s20051251
[5] Masikini M, Chowdhury M, Nemraoui O (2020) Review—Metal Oxides: Application in Exhaled Breath Acetone Chemiresistive Sensors. Journal of The Electrochemical Society 167 037537 https://doi.org/10.1149/1945-7111/ab64bc.
[6] Rowley WR, Bezold C, Arikan Y, Byrne E, Krohe S (2017) Diabetes 2030: Insights from Yesterday, Today, and Future Trends. Population Health Management 20 6–12 https://doi.org/10.1089/pop.2015.0181.
[7] Jang C, Park JK, Lee HJ, Yun GH, Yook JG (2018) Temperature-corrected fluidic glucose sensor based on microwave resonator. Sensors (Switzerland) 18 1–12 https://doi.org/10.3390/s18113850.
[8] Classification and diagnosis of diabetes: Standards of medical care in Diabetes-2018, Diabetes Care. 41 (2018) S13–S27. https://diabetesjournals.org/care/article/41/Supplement_1/S13/30088/2-Classification-and-Diagnosis-of-Diabetes
[9] Köksal Atış Ş and Önder A (2020) Yeni Tanı Diyabetes Mellitus Hastalarında Sınıflandırma ve Tedavi Yönetimi. Hitit Medical Journal 3 (2020) 62–66
[10] WHO, Use of Glycated Haemoglobin (HbA1c) in the Diagnosis of Diabetes Mellitus: Abbreviated Report of a WHO Consultation. Approved by the Guidelines Review Committee., World Health Organization. (2011) 299–309.
[11] I. Classification, Standards of medical care in diabetes-2014, Diabetes Care. 37 (2014) 14–80. https://doi.org/10.2337/dc14-S014.
[12] Abacı A, Böber E, Büyükgebiz A (2007) Tip 1 Diyabet. Güncel Pediatri 5 1–10 https://dergipark.org.tr/en/pub/pediatri/667492.
[13] Mishra BK (2013) Chemistry of Diabetes and its Impact. Academic Voices: A Multidisciplinary Journal 2 16–22 https://doi.org/10.3126/av.v2i1.8279.
[14] Yuan Y, Chen Z, Zhao X, Sun M, Li Y, Wang Z, Wang C (2017) Continuous Monitoring of Breath Acetone, Blood Glucose and Blood Ketone in 20 Type 1 Diabetic Outpatients Over 30 Days. Journal of Analytical & Bioanalytical Techniques 08 https://doi.org/10.4172/2155-9872.1000386.
[15] Güntner AT, Kompalla JF, Landis H, Theodore SJ, Geidl B, Sievi NA, Kohler M, Pratsinis SE, Gerber PA (2018) Guiding ketogenic diet with breath acetone sensors. Sensors (Switzerland) 18 1–12 https://doi.org/10.3390/s18113655
[16] Wang C, Mbi A, Shepherd M (2010)A study on breath acetone in diabetic patients using a cavity ringdown breath analyzer: Exploring correlations of breath acetone with blood glucose and glycohemoglobin A1C. IEEE Sensors Journal 10 54–63 https://doi.org/10.1109/JSEN.2009.2035730
[17] Musa-Veloso K, Likhodii SS, Rarama E, Benoit S, Liu YMC, Chartrand D, Curtis R, Carmant L, Lortie A, Comeau FJE, Cunnane SC (2006) Breath acetone predicts plasma ketone bodies in children with epilepsy on a ketogenic diet. Nutrition 22 1–8 https://doi.org/10.1016/j.nut.2005.04.008
[18] Puchalska P and Crawford PA (2017) Multi-dimensional Roles of Ketone Bodies in Fuel Metabolism, Signaling, and Therapeutics. Cell Metabolism 25 262–284 https://doi.org/10.1016/j.cmet.2016.12.022
[19] Güntner AT, Sievi NA, Theodore SJ, Gulich T, Kohler M, Pratsinis SE (2017) Noninvasive Body Fat Burn Monitoring from Exhaled Acetone with Si-doped WO3-sensing Nanoparticles. Analytical Chemistry 89 10578–10584 https://doi.org/10.1021/acs.analchem.7b02843
[20] Wang Z and Wang C (2013) Is breath acetone a biomarker of diabetes? A historical review on breath acetone measurements. Journal of Breath Research 7 https://doi.org/10.1088/1752-7155/7/3/037109
[21] Bovey F, Cros J, Tuzson B, Seyssel K, Schneiter P, Emmenegger L, Tappy L (2018) Breath acetone as a marker of energy balance: an exploratory study in healthy humans. Nutrition and Diabetes 8 https://doi.org/10.1038/s41387-018-0058-5
[22] Afreen S and Zhu JJ (2019) Rethinking EBAD: Evolution of smart noninvasive detection of diabetes. TrAC - Trends in Analytical Chemistry 118 477–487 https://doi.org/10.1016/j.trac.2019.06.011
[23] Konvalina G and Haick H (2014) Sensors for Breath Testing : From Nanomaterials to Comprehensive Disease Sensors for Breath Testing : From Nanomaterials to Comprehensive Disease Detection. Accounts of Chemical Research 47 1 66-76 https://doi.org/10.1021/ar400070m
[24] Rydosz A (2018) Sensors for enhanced detection of acetone as a potential tool for noninvasive diabetes monitoring. Sensors (Switzerland) 18 (2018) 1–14 https://doi.org/10.3390/s18072298
[25] Rydosz A (2015) A negative correlation between blood glucose and acetone measured in healthy and type 1 diabetes mellitus patient breath. Journal of Diabetes Science and Technology 9 881–884 https://doi.org/10.1177/1932296815572366
[26] Diskin AM, Španěl P, Smith D (2003) Time variation of ammonia, acetone, isoprene and ethanol in breath:

A quantitative SIFT-MS study over 30 days. Physiological Measurement 24 107–119 https://doi.org/10.1088/0967-3334/24/1/308
[27] Wang X, Qin H, Pei J, Chen Y, Li L, Xie J, Hu J (2016)Sensing performances to low concentration acetone for palladium doped LaFeO3 sensors. Journal of Rare Earths 34 704–710. https://doi.org/10.1016/S1002-0721(16)60082-0.
[28] Amann A and Smith D (2013) Volatile Biomarkers: Non-Invasive Diagnosis in Physiology and Medicine. Elsevier. https://doi.org/10.1016/C2012-0-01274-4
[29] Deng C, Zhang J, Yu X, Zhang W, Zhang X (2004) Determination of acetone in human breath by gas chromatography–mass spectrometry and solid-phase microextraction with on-fiber derivatization. Journal of Chromatography B 810 269–275 https://doi.org/10.1016/j.jchromb.2004.08.013
[30] Fergus JW, (2007)Perovskite oxides for semiconductor-based gas sensors. Sensors and Actuators B: Chemical 123 1169–1179 https://doi.org/10.1016/j.snb.2006.10.051
[31] Shankar P and Rayappan JBB (2015) Gas sensing mechanism of metal oxides: The role of ambient atmosphere, type of semiconductor and gases - A review. Science Letters Journal 4 126 http://www.cognizure.com/scilett.aspx?p=200638572
[32] Minh TDC, Blake DR, Galassetti PR (2012) The clinical potential of exhaled breath analysis for diabetes mellitus. Diabetes Research and Clinical Practice 97 195–205. https://doi.org/10.1016/j.diabres.2012.02.006
[33] Miekisch W, Schubert JK, Noeldge-Schomburg GFE (2004) Diagnostic potential of breath analysis - Focus on volatile organic compounds. Clinica Chimica Acta 347 25–39 https://doi.org/10.1016/j.cccn.2004.04.023
[34] Lourenço C and Turner C (2014) Breath Analysis in Disease Diagnosis: Methodological Considerations and Applications. Metabolites 4 465–498 https://doi.org/10.3390/metabo4020465
[35] Li J, Smeeton TM, Zanola M, Barrett J, Berryman-Bousquet V (2018) A compact breath acetone analyser based on an ultraviolet light emitting diode. Sensors and Actuators B: Chemical 273 76–82 https://doi.org/10.1016/j.snb.2018.05.114
[36] Prabhakar A, Quach A, Zhang H, Terrera M, Jackemeyer D, Xian X, Tsow F, Tao N, Forzani ES (2015) Acetone as biomarker for ketosis buildup capability - A study in healthy individuals under combined high fat and starvation diets. Nutrition Journal 14 https://doi.org/10.1186/s12937-015-0028-x
[37] King J, Kupferthaler A, Unterkofler K, Koc H, Teschl S, Teschl G, Miekisch W, Schubert J, Hinterhuber H, Amann A (2009) Isoprene and acetone concentration profiles during exercise on an ergometer Journal of Breath Research 3 027006 https://doi.org/10.1088/1752-7155/3/2/027006
[38] Blaikie TPJ, Edge JA, Hancock G, Lunn D, Megson C, Peverall R, Richmond G, Ritchie GAD, Taylor D (2014) Comparison of breath gases, including acetone, with blood glucose and blood ketones in children and adolescents with type 1 diabetes. Journal of Breath Research 8 046010 https://doi.org/10.1088/1752-7155/8/4/046010
[39] Do JS and Wang SH (2013) On the sensitivity of conductimetric acetone gas sensor based on polypyrrole and polyaniline conducting polymers. Sensors and Actuators B: Chemical 185 39–46 https://doi.org/10.1016/j.snb.2013.04.080
[40] Liu S, Zhang F, Li H, Chen T, Wang Y (2012) Acetone detection properties of single crystalline tungsten oxide plates synthesized by hydrothermal method using cetyltrimethyl ammonium bromide supermolecular template. Sensors and Actuators B: Chemical 162 259–268 https://doi.org/10.1016/j.snb.2011.12.076
[41] Huang Z, Zhang A, Zhang Q, Pan S, Cui D (2019) Electrochemical Biosensor Based on Dewdrop-Like Platinum Nanoparticles-Decorated Silver Nanoflowers Nanocomposites for H 2 O 2 and Glucose Detection. Journal of The Electrochemical Society 166 B1138–B1145 https://doi.org/10.1149/2.0471913JES/XML
[42] Staden RIS, Popa-Tudor I, Ionescu-Tirgoviste C, Stoica RA, Magerusan L (2019) Molecular Enantiorecognition of D- and L-Glucose in Urine and Whole Blood Samples. Journal of The Electrochemical Society 166 B3109–B3115 https://doi.org/10.1149/2.0211909JES/XML
[43] IDF, Eighth edition 2017, 2017. https://www.idf.org/aboutdiabetes/type-2-diabetes.html.
[44] Makaram P, Owens D, Aceros J (2014) Trends in Nanomaterial-Based Non-Invasive Diabetes Sensing Technologies. Diagnostics 4 27–46 https://doi.org/10.3390/diagnostics4020027
[45] Standards of medical care in diabetes-2010, Diabetes Care. 33 (2010). https://doi.org/10.2337/dc10-S011.
[46] Alonso M and Sanchez JM (2013) Analytical challenges in breath analysis and its application to exposure monitoring. TrAC - Trends in Analytical Chemistry 44 78–89 https://doi.org/10.1016/j.trac.2012.11.011
[47] Rooth G and Ostenson S (1966) Acetone in alveolar air, and the control of diabetes. Lancet 2 1102–1105. https://doi.org/10.1016/s0140-6736(66)92194-5
[48] Tassopoulos CN, Barnett D, Fraser TR (1969) Breath-acetone and blood-sugar measurements in diabetes. Lancet 293 1282–1286 https://doi.org/10.1016/s0140-6736(69)92222-3
[49] Kim KH, Jahan SA, Kabir E (2012) A review of breath analysis for diagnosis of human health. TrAC - Trends in Analytical Chemistry 33 1–8 https://doi.org/10.1016/j.trac.2011.09.013
[50] Kupferthaler A, King J, Amann A, Hinterhuber H, Hackner H, Hogl B (2010) Acetone and isoprene concentration profiles in normal human sleep. Memo - Magazine of European Medical Oncology 3 6–7

http://ovidsp.ovid.com/ovidweb.cgi?T=JS&PAGE=reference&D=emed11&NEWS=N&AN=70264318
[51] Saasa V, Malwela V, Beukes M, Mokgotho M, Liu CP, Mwakikunga B (2018) Sensing Technologies for Detection of Acetone in Human Breath for Diabetes Diagnosis and Monitoring. Diagnostics 8 12 https://doi.org/10.3390/diagnostics8010012
[52] Tomer VK, Singh K, Kaur H, Shorie M, Sabherwal P (2017) Rapid acetone detection using indium loaded WO3/SnO2 nanohybrid sensor. Sensors and Actuators B: Chemical 253 703–713 https://doi.org/10.1016/j.snb.2017.06.179
[53] Hung CM, Le DTT, Van Hieu N (2017) On-chip growth of semiconductor metal oxide nanowires for gas sensors: A review. Journal of Science: Advanced Materials and Devices 2 263–285 https://doi.org/10.1016/j.jsamd.2017.07.009
[54] Wong YC, Ang BC, Haseeb ASMA, Baharuddin AA, Wong YH (2020) Review—Conducting Polymers as Chemiresistive Gas Sensing Materials: A Review. Journal of The Electrochemical Society 167 037503 https://doi.org/10.1149/2.0032003jes
[55] Righettoni M, Amann A, Pratsinis SE (2015) Breath analysis by nanostructured metal oxides as chemo-resistive gas sensors. Materials Today 18 163–171 https://doi.org/10.1016/j.mattod.2014.08.017
[56] Korotcenkov G (2007) Metal oxides for solid-state gas sensors: What determines our choice?. Materials Science and Engineering B: Solid-State Materials for Advanced Technology 139 1–23 https://doi.org/10.1016/j.mseb.2007.01.044
[57] Wetchakun K, Samerjai T, Tamaekong N, Liewhiran C, Siriwong C, Kruefu V, Wisitsoraat A, Tuantranont A, Phanichphant S (2011) Semiconducting metal oxides as sensors for environmentally hazardous gases. Sensors and Actuators B: Chemical 160 580–591 https://doi.org/10.1016/j.snb.2011.08.032
[58] Li SM, Zhang LX, Zhu MY, Ji GJ, Zhao LX, Yin J, Bie LJ (2017) Acetone sensing of ZnO nanosheets synthesized using room-temperature precipitation. Sensors and Actuators B: Chemical 249 611–623 https://doi.org/10.1016/j.snb.2017.04.007
[59] Navale ST, Yang ZB, Liu C, Cao PJ, Patil VB, Ramgir NS, Mane RS, Stadler FJ (2018) Enhanced acetone sensing properties of titanium dioxide nanoparticles with a sub-ppm detection limit. Sensors and Actuators B: Chemical 255 1701–1710 https://doi.org/10.1016/j.snb.2017.08.186
[60] Giang HT, Duy HT, Ngan PQ, Thai GH, Thu DTA, Thu DT, Toan NN (2011) Hydrocarbon gas sensing of nano-crystalline perovskite oxides LnFeO 3 (Ln = La, Nd and Sm). Sensors and Actuators B: Chemical 158 246–251 https://doi.org/10.1016/j.snb.2011.06.013
[61] Song P, Wang Q, Zhang Z, Yang Z (2010) Synthesis and gas sensing properties of biomorphic LaFeO3 hollow fibers templated from cotton. Sensors and Actuators B: Chemical 147 248–254 https://doi.org/10.1016/j.snb.2010.03.006
[62] Fan K, Qin H, Wang L, Ju L, Hu J (2013) CO2 gas sensors based on La1-xSrxFeO 3 nanocrystalline powders. Sensors and Actuators B: Chemical 177 265–269 https://doi.org/10.1016/j.snb.2012.11.004
[63] Naseri M and Ghasemi R (2016) Structure and physical properties of Fe6 O8/ba Fe6 O11 nanostructure. Journal of Magnetism and Magnetic Materials 406 200–206 https://doi.org/10.1016/j.jmmm.2016.01.019
[64] Anajafi Z, Naseri M, Neri G (2020) Acetone sensing behavior of p-SmFeO3/n-ZnO nanocomposite synthesized by thermal treatment method. Sensors and Actuators B: Chemical 304 https://doi.org/10.1016/j.snb.2019.127252
[65] Hao P, Lin Z, Song P, Yang Z, Wang Z (2020) Hydrothermal preparation and acetone-sensing properties of Ni-doped porous LaFeO3 microspheres. Journal of Materials Science: Materials in Electronics 31 6679–6689 https://doi.org/10.1007/s10854-020-03224-x
[66] Zhang YH, Li YL, Gong FL, Xie KF, Liu M, Zhang HL, Fang SM (2020) Al doped narcissus-like ZnO for enhanced NO2 sensing performance: An experimental and DFT investigation. Sensors and Actuators B: Chemical 305 127489 https://doi.org/10.1016/j.snb.2019.127489
[67] Ma L, Ma SY, Shen XF, Wang TT, Jiang XH, Chen Q, Qiang Z, Yang HM, Chen H (2018) PrFeO3 hollow nanofibers as a highly efficient gas sensor for acetone detection. Sensors and Actuators B: Chemical 255 2546–2554 https://doi.org/10.1016/j.snb.2017.09.060
[68] Pei S, Ma S, Xu X, Xu X, Almamoun O (2021) Modulated PrFeO3 by doping Sm3+ for enhanced acetone sensing properties. Journal of Alloys and Compounds 856 158274 https://doi.org/10.1016/j.jallcom.2020.158274
[69] Bulut U, Oyku Sayin V, Altin Y, Can Cevher S, Cirpan A, Celik Bedeloglu A, Soylemez S (2023) A flexible carbon nanofiber and conjugated polymer-based electrode for glucose sensing. Microchemical Journal 184 108148. https://doi.org/10.1016/j.microc.2022.108148
[70] Virji S, Huang J, Kaner RB, Weiller BH (2004) Polyaniline nanofiber gas sensors: Examination of response mechanisms. Nano Letters 4 491–496 https://doi.org/10.1021/nl035122e
[71] Ding B, Wang M, Yu J, Sun G (2009) Gas sensors based on electrospun nanofibers. Sensors 9 1609–1624 https://doi.org/10.3390/s90301609
[72] Gupta N, Sharma S, Mir IA, Kumar D (2006) Advances in sensors based on conducting polymers. Journal

of Scientific and Industrial Research 65 549–557
[73] Wang Y, Liu A, Han Y, Li T (2020) Sensors based on conductive polymers and their composites: a review. Polymer International 69 7–17 https://doi.org/10.1002/pi.5907
[74] Pirsa S (2017) Chemiresistive gas sensors based on conducting polymers. In Khosrow-Pour M (ed) Materials Science and Engineering: Concepts, Methodologies, Tools, and Applications, Engineering Science Reference, 1–3, pp. 543–574 https://doi.org/10.4018/978-1-5225-1798-6.ch022
[75] Tang P, Xie X, Chen H, Lv C, Ding Y (2019) Synthesis of Nanoparticulate PrFeO3 by Sol–Gel Method and its Visible-Light Photocatalytic Activity. Ferroelectrics 546 181–187 https://doi.org/10.1080/00150193.2019.1592470
[76] Jin LN, Shao F, Jin C, Zhang JN, Liu P, Guo MX, Bian SW (2017) High-performance textile supercapacitor electrode materials enhanced with three-dimensional carbon nanotubes/graphene conductive network and in situ polymerized polyaniline. Electrochimica Acta 249 387–394 https://doi.org/10.1016/j.electacta.2017.08.035
[77] Kim NH, Choi SJ, Kim SJ, Cho HJ, Jang JS, Koo WT, Kim M, Kim ID (2016) Highly sensitive and selective acetone sensing performance of WO3 nanofibers functionalized by Rh2O3 nanoparticles. Sensors and Actuators B: Chemical 224 185–192 https://doi.org/10.1016/j.snb.2015.10.021
[78] Tijare SN, Bakardjieva S, Subrt S, Joshi MV, Rayalu SS, Hishita S, Labhsetwar N (2014) Synthesis and visible light photocatalytic activity of nanocrystalline PrFeO 3 perovskite for hydrogen generation in ethanol-water system. Journal of Chemical Sciences 126 517–525 https://doi.org/10.1007/s12039-014-0596-x
[79] Altin Y and Celik Bedeloglu (2021) A Polyacrylonitrile/polyvinyl alcohol-based porous carbon nanofiber electrodes for supercapacitor applications. International Journal of Energy Research 45 16497–16510 https://doi.org/10.1002/ER.6896
[80] Chireh M and Naseri M (2019) Effect of calcination temperature on the physical properties of LiFe 5 O 8 nanostructures. Advanced Powder Technology 30 952–960 https://doi.org/10.1016/j.apt.2019.02.009
[81] Zhang H, Xiao J, Chen J, Zhang L, Zhang Y, Jin P (2022) Au modified PrFeO3 with hollow tubular structure can be efficient sensing material for H2S detection. Frontiers in Bioengineering and Biotechnology 10 1–12 https://doi.org/10.3389/fbioe.2022.969870
[82] Mirzaei A, Majhi SM, Kim HW, Kim SS (2022) Metal oxide-based nanofibers and their gas-sensing applications. In Esposito V and MArani D (ed) Metal Oxide-Based Nanofibers and Their Applications, Elsevier, pp. 139–158 https://doi.org/10.1016/B978-0-12-820629-4.00008-4